Int. J. Heat Mass Transfer. Vol. 25, No. 9, pp. 1377–1382, 1982
Printed in Great Britain

0017–9310/82/091377–06 $03.00/0
Pergamon Press Ltd.

IMPINGEMENT OF A CIRCULAR JET WITH AND WITHOUT CROSS FLOW

R. J. GOLDSTEIN and A. I. BEHBAHANI
Department of Mechanical Engineering, University of Minnesota, Minneapolis, MN 55455, U.S.A.

(*Received* 5 *April* 1982)

Abstract—Measurements are reported for the local heat transfer to an impinging air jet with and without a cross flow of air. At large jet-to-plate spacing the cross flow diminishes the peak heat transfer coefficient; at a smaller spacing cross flow can increase the peak heat transfer coefficient. A correlation is obtained for the average heat transfer in the absence of cross flow.

NOMENCLATURE

- A_j, jet exit area [m^2];
- C_p, specific heat of air;
- D, jet diameter (12.7 mm in experiment);
- h, local heat transfer coefficient, $q_w/(T_w - T_{ad})$;
- h', local heat transfer coefficient, $q_w/(T_w - T_j^\circ)$;
- h_∞, local heat transfer coefficient in the absence of jet flow, $q_w/(T_w - T_\infty^\circ)$;
- k, thermal conductivity of air;
- M, blowing rate, $(\rho_j U_j)/(\rho_\infty U_\infty)$;
- m_j, jet mass flow rate [kg s^{-1}];
- Nu, local Nusselt number, $(hD)/k$;
- Nu', local Nusselt number, $(h'D)/k$;
- Nu_0, stagnation (peak) Nusselt number;
- Nu_∞, local Nusselt number in the absence of jet, $(h_\infty D)/k$;
- $\overline{Nu}$, Nusselt number averaged over area from $R = 0$ to $R = x_i$;
- q, heat input per unit area;
- Re_j, jet Reynolds number, $(U_j D)/\nu_j$;
- r, recovery factor, $(T_{ad} - T_j^s)/(U_j^2/2C_p)$;
- R, radial distance from geometrical center of jet;
- T_{ad}, adiabatic wall temperature [°C];
- T_j^s, jet static temperature [°C];
- T_j°, jet total temperature [°C];
- T_R, room temperature [°C];
- T_w, wall temperature [°C];
- T_∞°, mainstream total temperature [°C];
- U_∞, mainstream velocity [m s^{-1}];
- U_j, jet velocity, $m_j/(\rho_j A_j)$ [m s^{-1}];
- X, streamwise direction ($x = 0$ is the location of the jet's geometrical center);
- X_i, distance to both sides of $x = 0$ over which average Nusselt number is calculated;
- X_{Nu_0}, downstream location where maximum Nusselt number occurs;
- z, lateral position across span from geometrical center of jet (all data presented herein were obtained at $z = 0$).

Greek symbols

- ν, kinematic viscosity;
- ρ, density.

Subscripts

- j, jet;
- ∞, free stream.

INTRODUCTION

IMPINGING jets are often used to heat or cool a surface [1]. Specific applications include cooling of the leading edge of turbine blades, cooling of electrical equipment, and paper drying.

One of the earliest works on jet impingement was conducted by Perry [2], who studied the effect of the angle of impingement on the average rate of heat transfer of a hot-air jet to a surface located at 8 nozzle diameters from the jet exit. Gardon and Cobonpue [3] investigated the variation of heat transfer rate with jet-to-plate spacing distance and observed a maximum heat transfer coefficient at a jet-to-plate distance of between 6 and 7 jet diameters. Tataoka, Komai and Nakamura [4] found the maximum heat transfer coefficient at a jet-to-plate distance of 6 jet diameters. Gaunter, Livingood and Hrycak [5] surveyed the flow characteristics of a single turbulent jet impinging on a flat plate and suggest that to maximize the heat transfer coefficient, a jet-to-plate distance of 6 jet diameters be used.

The effect of a cross flow on the heat transfer characteristics of impinging jets has been studied by several investigators. Kercher and Tabakoff [6] measured the influence of spent air on the average heat transfer to a square array of round jets in a semi-closed environment and concluded that increasing cross flow decreases the heat transfer performance. Metzger *et al.* [7] and Florschuetz, Berry and Metzger [8] studied the heat transfer characteristics of in-line and staggered arrays of jets with a cross-flow of spent air. Metzger and Korstad [9] measured the average heat transfer from a rectangular surface to a line of circular air jets with an imposed cross flow. They observed a decrease in average heat transfer coefficient with cross flow upstream of impingement. Bouchez and Goldstein [9] measured local adiabatic wall temperatures and local heat transfer coefficients for a circular jet at jet-to-plate spacings of 6 and 12 jet diameters in the presence of a cross flow of constant velocity of 12 m s^{-1}; they found that the experimental data could be correlated using adiabatic wall temperatures, which had also been suggested in ref. [2]. Sparrow, Goldstein and Rouf [10] added to the results of ref. [9] with measurements at jet-to-plate spacings of 10, 8, 7, 5, 4 and 3 jet diameters. They found the highest heat transfer coefficients at jet-to-plate spacings between 5 and 6 jet diameters for high jet Reynolds numbers ($Re_j > 70\,000$) and at a jet-to-plate spacing of $3D$ for low Reynolds numbers ($Re \simeq 35\,000$) with cross flow.

In the present study, the work of ref. [9] is extended by measuring local heat transfer to a circular air jet with jet-to-plate spacings of 6 and 12 diameters in the presence of a cross flow of 8.5 m s^{-1} and 16.5 m s^{-1}. In addition local heat transfer coefficients are measured with zero cross flow in the same experimental system.

EXPERIMENTAL APPARATUS AND OPERATIONAL PROCEDURE

The experiments were carried out in a wind tunnel with a rectangular cross section 20.32 cm wide by 15.24 cm high, and a total length of 114 cm [Fig. 1(a)]. Room air is drawn into the wind tunnel by a squirrel cage fan located at the exit of the tunnel. The boundary layer is rendered turbulent by a trip 1.91 cm upstream of the test plate.

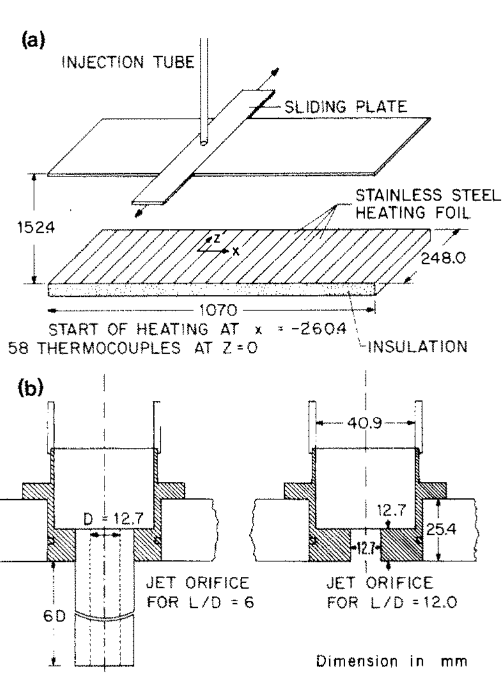

FIG. 1(a). Experimental apparatus and (b) jet orifice plate.

The air for the jet is supplied by the building compressor. After filtering and regulation, it is metered by a thin replaceable orifice plate. Then, with the aid of an electrical heater, the air is heated to the desired temperature before exiting from the jet orifice. Figure 1(b) shows the jet orifice configuration for $L/D = 6$ and 12.

The test plate is made of thin textolite with styrofoam backing. Stainless steel heating foils (25.4 μm thick) are bounded on the textolite and 30 gauge iron–constantan thermocouples are imbedded in the test plate in contact with the heating foils.

For tests with cross flow, the jet exit mass flow and the cross flow are adjusted to the desired values. During each run, the jet flow is heated so that

$$T_j^{\circ} \simeq T_r^{\circ}. \tag{1}$$

In tests of jet impingement in still air, the walls of the test section are removed, and the secondary flow is heated so that

$$T_j^{\circ} \simeq T_R. \tag{2}$$

Each test run is done in two parts. First, the temperature distribution on the test plate is measured when the wall heat flux is zero. This provides the adiabatic wall temperatures. Then temperatures are measured on the test plate after the heating foils have been energized.

RESULTS

Experimental results are presented in terms of the Nusselt number

$$Nu = (hD)/k \tag{3}$$

where D is the jet diameter and k is the thermal conductivity of air evaluated at the film temperature, $(T_w + T_r)/2$. The heat transfer coefficient is defined as

$$h = \frac{q}{T_w - T_{ad}} \tag{4}$$

where q is the heat flow from the surface per unit area, T_w is the local wall temperature, and T_{ad} is the local adiabatic wall temperature measured when $q = 0$. The radiation and conduction losses from the plate are small; essentially all the energy input to the plate appears as convective heat flow from the surface. Use of $T_w - T_j^{\circ}$ as the driving force [i.e. $h' = q/(T_w - T_j^{\circ})$] instead of $T_w - T_{ad}$ in equation (4) would result in h being dependent on q and, for the conditions of the present test, reduce the magnitude of the heat transfer coefficient in the stagnation region.

This difference in the two Nusselt numbers, Nu and Nu', is apparent in Fig. 2 for $Re \simeq 121\,000$ and no cross flow. If the wall heat flux were such that $|(T_w - T_{aw})| \gg |(T_{aw} - T_j^{\circ})|$, the values of Nu' should approach those of Nu. At a lower jet Reynolds number (Fig. 2), when the total temperature in the jet is close to the

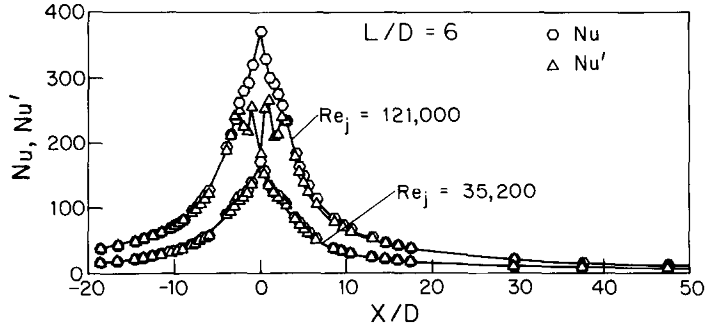

FIG. 2. Variation of local Nusselt number using different temperature differences in definition of the heat transfer coefficient.

recovery (adiabatic wall) temperature, there is little difference between the values of Nu and Nu'. This figure shows the importance of knowing the adiabatic wall temperature if results are to be obtained that can be used generally for a variety of conditions.

Figures 3 and 4 show the streamwise variation of the recovery factor, r, defined by

$$r = \frac{T_{ad} - T_j^{\circ}}{U_j^2/2C_p}. \tag{5}$$

For the sample runs the recovery factor varies from a value close to unity far upstream of the impingement region to a maximum occurring at the stagnation point; far downstream it is again close to unity. A minimum sometimes appears at $x/D \sim \pm 5$ particularly for $L/D = 6$. Although care was taken to equalize T_j° with T_{∞}° or T_R by heating the jet air flow, small variations in T_{∞}° or T_R with time could not be prevented. This produced some scatter in r at low jet Reynolds numbers.

The variation of local Nusselt number along the centerline (i.e. $z = 0$) of the test section is shown in Figs. 5 and 6 for jet-to-plate spacings of 12 and 6 diameters, respectively. The blowing parameters and jet Reynolds number are shown on these figures. On figures with cross flow, the Nusselt number corresponding to cross flow only (i.e. Nu_{∞} for $M = 0$) is also presented.

A common feature of the results for both spacings is that with cross flow the symmetry of the jet is destroyed. The location of the maximum local Nusselt number moves downstream from the geometrical center of the jet ($x = 0$) as M decreases. The location of the maximum (x_{Nu_0}) is presented as a function of M in Table 1.

Turning specifically to the results for $L/D = 12$, consider first the jet impingement heat transfer in the absence of cross flow [Fig. 5(a)]. Nu is a maximum at the center of the jet and decreases for $|x| > 0$. The heat transfer coefficient distribution on the surface should be radially symmetric in the absence of cross flow. The stagnation Nusselt number, Nu_0, increases with increasing Re_j as a result of increasing jet centerline velocity.

Figures 5(b) and (c) show Nu with $L/D = 12$ for cross flows of 8.5 m s^{-1} and 16.6 m s^{-1}, respectively. On each figure, upstream of the jet, Nu is seen to have a value equal to that for the mainstream flow in the absence of jet (i.e. Nu_{∞}). Upstream approaching the stagnation region the Nu with cross flow is less than that observed for the same Re_j without cross flow; the mainstream flow can impede the back-flowing jet. Close to the stagnation region, the effect of the jet is felt strongly and Nu increases with x until it reaches a maximum at the stagnation point*. At larger positive

* The stagnation point is generally used here to describe the location of the maximum in heat transfer coefficient. This is probably close to the flow stagnation point.

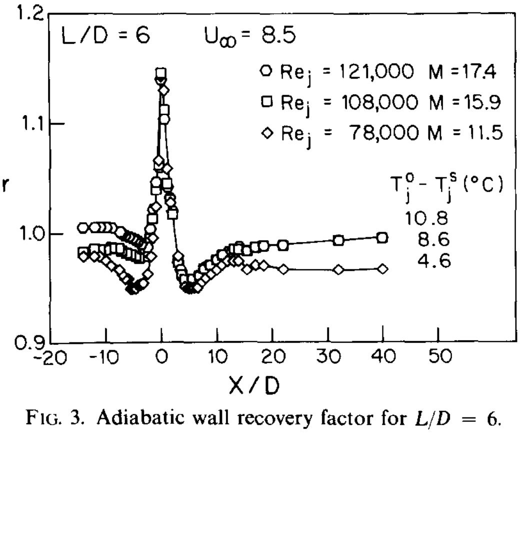

FIG. 3. Adiabatic wall recovery factor for $L/D = 6$.

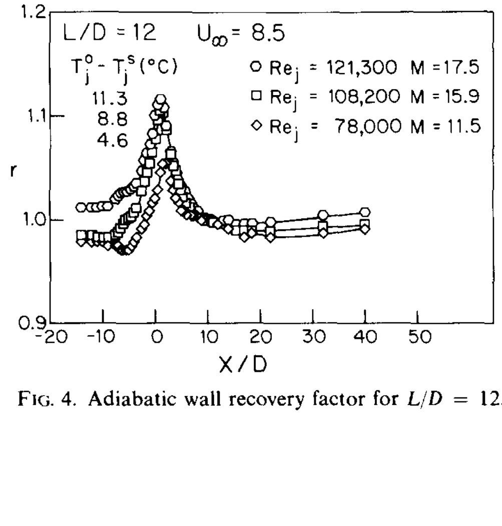

FIG. 4. Adiabatic wall recovery factor for $L/D = 12$.

Table 1. Values of Nu_0

		$L/D = 6$					$L/D = 12$		
U_∞	M	Re_j	Nu_0	X_{Nu_0}/D	U_∞	M	Re_j	Nu_0	X_{Nu_0}/D
		121 000	370	0			120 500	245	0
		109 000	343	0			108 100	217	0
0	∞	77 000	276	0	0	∞	76 200	186	0
		35 200	172	0			35 100	170	0
	17.4	121 000	412	0		17.5	121 300	218	1
	15.9	108 000	360	0		15.9	108 200	193	1
8.5	11.5	78 600	278	0	8.5	11.5	78 000	150	2
	4.9	33 400	102	2		5.1	34 300	27	20
	9.2	120 000	370	0.5		9.0	120 800	178	3
16.6	8.3	108 500	307	0.5	16.6	8.3	107 000	149	3.5
	5.8	78 300	218	0.5		5.9	76 000	58	14

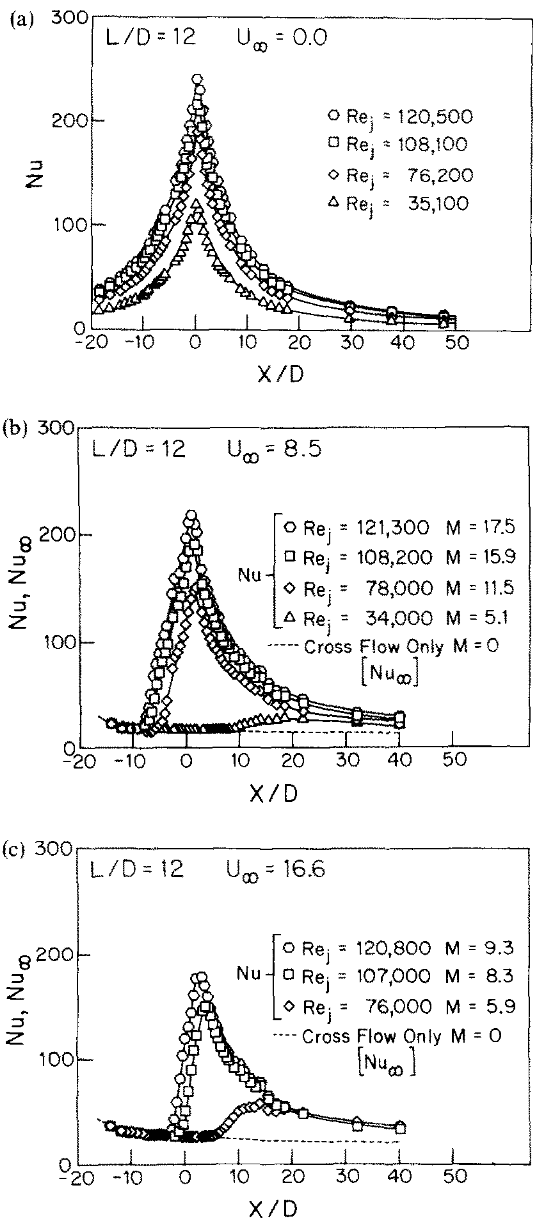

FIG. 5. Local Nusselt number for $L/D = 12$.

Table 2. Comparison of $\overline{Nu}/Re_j^{0.6}$ for $L/D = 6$

x_i/D	Present study	ref. [15]
3	0.2238	0.2197
6	0.16301	0.1552

values of x, Nu decreases as the influence of the jet decreases with distance from stagnation, and the boundary layer thickness increases. Comparing Figs. 5(a), (b) and 5(c), increasing cross flow causes the stagnation region Nu to decrease. At higher relative mainstream velocity, the external flow deflects the jet further downstream and mixes more with the jet, causing the approach velocity to the wall to decrease The higher mainstream velocity does, of course, produce larger heat transfer coefficients at far upstream and downstream locations.

The results for tests with jet-to-plate spacings of $L/D = 6$ are shown in Fig. 6. In the absence of cross flow [Fig. 6(a)], the maximum Nusselt number occurs at $X = 0$ with values higher than those at $L/D = 12$ for all Re_j due to higher arrival velocity. With cross flow [Figs. 6(b) and 6(c)], Nu_0 is larger for $M > 9$ than it is in the absence of cross flow. This increase is larger for larger values of M. The increase of Nu_0 with cross flow for $L/D = 6$ can be attributed to an increase in jet centerline turbulence intensity from the mixing of the cross-flowing stream. This effect is not observed for small values of M (Table 1).

All thermocouples were located on the centerline of the test section, and no off-centerline data were taken. However impingement of jets in still air should be radially symmetric, and the centerline data can be averaged to give the mean Nusselt number in the absence of cross flow

$$\overline{Nu} = \frac{2}{x_i^2}\int_0^{x_i} NuR\,\mathrm{d}R. \qquad (6)$$

This integral was determined numerically for $x_i/D =$

0.5, 1, 2, 3, 6, 12, 18 and 32. At the two values of L/D used, the experimental data are satisfactorily correlated by

$$\frac{\overline{Nu}}{Re_j^{0.6}} = \frac{1}{A + B\,(x/D)^n} \tag{7}$$

where $A = 3.329$, $B = 0.273$ and $n = 1.3$ when $L/D = 6$ and $A = 4.577$, $B = 0.4357$ and $n = 1.14$ when $L/D = 12$. Figure 7 shows this correlation of the experimental results.

COMPARISON OF RESULTS

Local heat transfer results are compared in Fig. 8 with the work of Kirzek, presented in Fig. 17 of ref. [14] and the work of den Ouden and Hoogendoorn [15]. Kirzek used mass transfer techniques with naphthalene, and a liquid crystal technique was used in ref. [15]. The present results are in good agreement with these earlier tests, although some difference exists

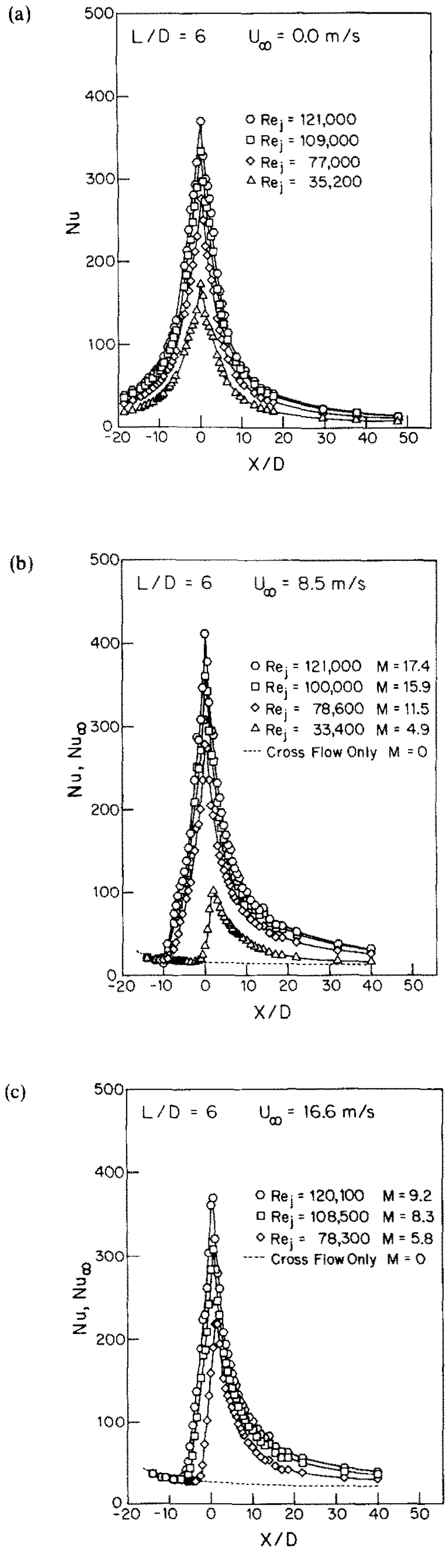

FIG. 6. Local Nusselt number for $L/D = 6$.

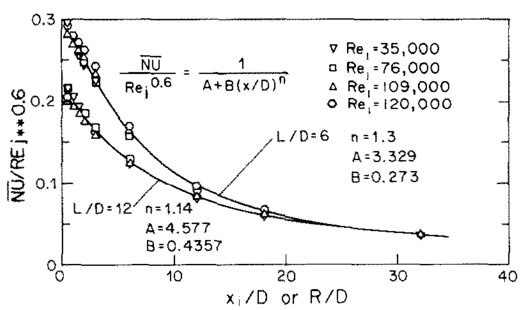

FIG. 7. Average Nusselt number correlation.

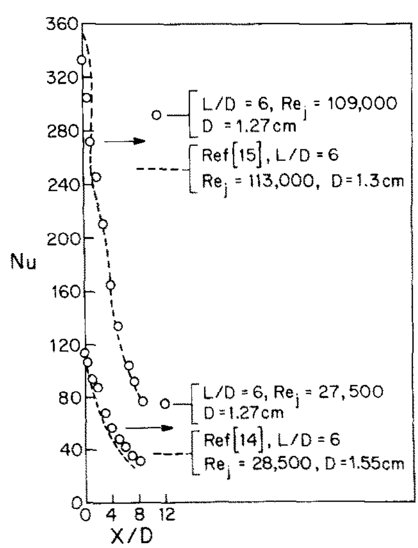

FIG. 8. Comparison of local Nusselt number with results of other investigators.

around the stagnation region. This may be due to different jet flow structures which result in different turbulence levels. Data of ref. [15] are averaged over $x_i/D = 3$ and 6 and, as shown in Table 2, agree well with the present results.

CONCLUDING REMARKS

For jets impringing normal to a surface, the maximum Nusselt number decreases with increasing cross flow for jet-to-plate spacing of 12. For jet-to-plate spacing of $L/D = 6$, the maximum Nusselt number increases with moderate cross flow when $M > 9$. At both spacings the peak Nusselt number moves downstream as the blowing rate decreases.

Acknowledgement—The research was supported by a grant from the Division of Engineering, Mathematics and Geo-Sciences of the U.S. Department of Energy.

REFERENCES

1. H. Martin, Heat and mass transfer between impinging gas jets and solid surfaces, *Advances in Heat Transfer* (edited by T. Irvine and J. P. Hartnett) Vol. 13, pp. 1–60. Academic Press, New York (1977).
2. K. P. Perry, Heat transfer by convection from a hot gas jet to a plane surface, *Proc. Mech. Eng. Inst.* **168**, 775–784 (1954).
3. R. Gardon and J. Cobonpue, Heat transfer between a flat plate and jets of air impinging on it, International Heat Transfer Conference, Part II, pp. 454–460 (1961).
4. K. Tataoka, T. Komai and G. Nakamura, Enhancement mechanics of mass transfer in a turbulent impinging jet for high Schmidt number, ASME Paper No. 78-HT-5.
5. J. W. Gauntner, N. B. Livingood and P. Hrycak, Survey of literature on flow characteristics of a single turbulent jet impinging on a flat plate, NASA TN D-5652 (1970).
6. D. M. Kercher and W. Tabakoff, Heat transfer by a square array of round jets impinging perpendicular to a flat surface including the effect of spent air, *J. Engng Power* **22**, 73–82 (1970).
7. D. E. Metzger, L. W. Florschuetz, D. I. Takeuchi, R. D. Behee and R. A. Berry, Heat transfer characteristics for inline and staggered arrays of circular jets with cross-flow of spent air, *Trans. Am. Soc. Mech. Engrs*, Series C, *J. Heat Transfer* **101**, 526–531 (1979).
8. L. W. Florschuetz, R. A. Berry and D. E. Metzger, Periodic streamwise variations of heat transfer coefficients for inline and staggered arrays of circular jets with crossflow of spent air, ASME Paper No. 79-WA/GT-11.
9. D. E. Metzger and R. J. Korstad, Effect of crossflow on impingement heat transfer, *J. Engng Power* **94**, 35–42 (1972).
10. J. P. Bouchez and R. J. Goldstein, Impingement cooling from a circular jet in a cross flow, *Int. J. Heat Mass Transfer* **18**, 719–730 (1975).
11. E. M. Sparrow, R. J. Goldstein and M. A. Rouf, Effect of nozzle-surface separation distance on impingement heat transfer for a jet in a cross flow, *Trans. Am. Soc. Mech. Engrs*, Series C, *J. Heat Transfer* **97**, 528–533 (1975).
12. J. P. Bouchez, Heat transfer to an impinging circular jet in a cross flow, Ph.D. thesis, Department of Mechanical Engineering, University of Minnesota (1973).
13. M. A. Rouf, Effect of separation distance on the local impingement heat transfer coefficient in the presence of cross flow, M.S. thesis, Department of Mechanical Engineering, University of Minnesota (1975).
14. D. E. Metzger, T. Yamashita and C. W. Jenkins, Impingement cooling of convave surfaces with lines of circular air jets, *J. Engng Power* **91**, 149–158 (1969).
15. C. J. Hoogendoorn and C. den Ouden, Local convective heat transfer coefficients for jets impinging on a flat plate; experiments using a liquid crystal technique, *Heat Transfer 1974 (Proceedings of the Fifth International Heat Transfer Conference, Tokyo)*, Vol. 5, pp. 293–297. The Japan Society of Mechanical Engineers/The Society of Chemical Engineers (1974).

IMPACT D'UN JET CIRCULAIRE AVEC OU SANS ECOULEMENT TRANSVERSAL

Résumé—On décrit des mesures du transfert thermique local d'un jet d'air incident avec ou sans écoulement transversal d'air. A grande distance entre base et plan, l'écoulement transversal diminue le pic du coefficient de transfert thermique; aux plus petites distances, l'écoulement transversal peut augmenter le pic. Une formule est obtenue pour le transfert thermique moyen en l'absence d'écoulement transversal.

AUFTREFFEN EINES ACHSENSYMMETRISCHEN FREISTRAHLS MIT UND OHNE QUERSTRÖMUNG

Zusammenfassung—Es wird über Messungen des örtlichen Wärmeübergangs beim Auftreffen eines Luftstrahls mit und ohne querströmende Luft berichtet.

Bei größen Abständen zwischen Düse und Platte vermindert die Querströmung den Höchstwert des Wärmeübergangskoeffizienten, während sie ihn bei kleineren Abständen erhöhen kann. Eine Beziehung für den mittleren Wärmeübergang ohne Querströmung wurde erhalten.

НИСПАДАЮЩАЯ КРУГЛАЯ СТРУЯ В УСЛОВИЯХ С ПОПЕРЕЧНЫМ ПОТОКОМ И БЕЗ НЕГО

Аннотация—Представлены результаты измерений локального теплопереноса к падающей струе воздуха при наличии поперечного потока воздуха и без него. В случае большого зазора между струей и пластиной поперечный поток уменьшает максимальный коэффициент теплопереноса; при меньшем зазоре поперечный поток может увеличивать максимальный коэффициент теплопереноса. Получено обобщенное соотношение для расчета средней величины теплового потока в случае отсутствия поперечного течения воздуха.